Chemical Engineering Science, Vol. 48, No. 8, pp. 1393–1404, 1993.
Printed in Great Britain.

0009–2509/93 $6.00 + 0.00

HEAT TRANSFER PROPERTIES OF A SCRAPED-SURFACE HEAT EXCHANGER IN THE TURBULENT FLOW REGIME

R. DE GOEDE† and E. J. DE JONG
Delft University of Technology, Laboratory for Process Equipment, Leeghwaterstraat 44, 2628 CA Delft, The Netherlands

(*Received* 11 *September* 1991; *accepted for publication* 21 *July* 1992)

Abstract—Heat transfer in scraped-surface heat exchangers processing turbulent flowing media has been modelled by combining a regular model for turbulent pipe flow with penetration theory to account for the disturbance of the thermal boundary layer by the scraper action. Comparison of the model with experimental data obtained with a bench scale unit revealed that the heat transfer coefficient depends more strongly on the rotational frequency of the scrapers than the model predicts. This phenomenon could be ascribed to the generation of vortices due to the scraper action, as has been confirmed by computer simulation as well as experimental flow visualization. Correction of the model for the occurrence of these vortices yielded a satisfying agreement between predicted and experimentally determined heat transfer coefficients.

1. INTRODUCTION

Scraped-surface heat exchangers are usually applied for (i) processing of viscous materials, where the scraper action serves to increase heat transfer, and (ii) processing crystallizing media, where the scraper mechanism is installed in order to prevent scaling, i.e. undesired growth of a crystal layer on the heat exchanger wall.

The application underlying the investigation described in this paper is the isolation of paraxylene. Industrial separation of paraxylene from its isomers (orthoxylene, metaxylene, ethylbenzene) is largely performed by crystallization, Technically occurring feedstocks usually contain about 20–25% paraxylene. Upon cooling such a mixture, crystallization initiates at ≈ -35°C. In general, cooling can be continuated down to -60°C. At lower temperatures, metaxylene cocrystallizes.

The process we have studied uses two crystallization stages (-45 and -60°C). Each stage consists of an adiabatic crystallizer and a cascade of scraped-surface heat exchangers in a recycle loop. In order to reduce the temperature difference between heat exchanger inlet and outlet temperatures, high flow rates are applied ($Re \approx 10^5$). The walls of the scraped-surface heat exchangers are the coldest spots in the process and, because of the relatively high supercooling present there, undesired crystal growth phenomena like scaling and dendritic growth occur. Also, superfluous nucleation might occur as a result of the high temperature drop near the walls.

All these crystal growth events have a negative influence on process economics and/or product quality. Scaling seriously hinders heat transfer because the scale layer introduces an additional resistance in the overall-heat transfer coefficient. Uncontrolled crystal growth often leads to inclusion of impurities and too high nucleation rates would result in a fine product, which causes difficulties at the solid–liquid separation stage. It will be obvious that control of the wall temperature in order to reduce or eliminate the undesired crystal growth events mentioned above would greatly contribute to improve product quality and process economics. Because, for a fixed production capacity, the heat flux through the walls and the bulk temperature are invariable, the only possibility of controlling the temperature at the heat exchanger wall is by manipulating the heat transfer coefficient.

The scope of this investigation can, therefore, be defined as to determine how the heat transfer coefficient depends on hydrodynamic conditions that, for given pieces of equipment and process medium, are fully defined by the volumetric throughput and rotational speed of the scraper. The objective is to obtain a useful tool for controlling the wall temperature and, hence, nucleation and growth behaviour at or near the wall. In order to achieve this, a mathematical model taking the influences of axial flow rate and scraper rotational speed into account has been developed. For experimental support, heat transfer coefficients were measured on a bench scale model of a scraped-surface heat exchanger using a C8 aromatic mixture as a test medium. Temperatures were kept between 0 and -20°C such that crystallization of paraxylene did not occur. Visualization of the flow pattern was carried out in an other device that represents a cross-sectional segment of a scraped-surface heat exchanger.

2. THEORY

2.1. *Literature survey*

Huggins (1931) was the first to use scrapers in vessels instead of stirrers. He found a strong enhancement of the heat transfer coefficient when viscous media were used. For non-viscous media, the effect of the scraper action on the heat transfer coefficient

†Present address: TNO, Institute of Environmental and Energy Technology, Laan van Westenenk 501, PO Box 342, 7300 AH Apeldoorn, The Netherlands.

proved to be less pronounced. Houlton (1944) investigated heat transfer between two water flows in a scraped-surface heat exchanger. The influence of flow and scraper frequency were measured. The overall heat transfer coefficients were in the order of 3000–7000 $W m^{-2} K^{-1}$. Skelland (1958) derived a correlation for the heat transfer coefficient based on dimensional analysis. The exponents were derived from experimental data. He used floating (i.e. not spring-loaded) scraper blades, which implies that there is no contact between the blade and the wall because of a stagnant layer in between. The presence of this layer may have a dramatic influence on the heat transfer coefficient when viscous media are being processed. Nearly all experiments have been performed in the transition region from laminar to turbulent flow, which complicates a theoretically based evaluation of the exponents. He found $\alpha \propto N^{0.17}$ and $\alpha \propto v^{0.4}$ for viscous media (oils, glycerol).

Only for water Skelland found $\alpha \propto N^{0.5}$ and $\alpha \propto v^{0.4}$. The rotational *Re* number for water indicates turbulent flow. The difference in exponents found for water and for the other media indicates the existence of different flow regimes. Latinen (1958) derived an expression for the heat transfer coefficient based on penetration theory, assuming a stagnant liquid layer to be present at the wall that completely mixes up with the bulk after being scraped off. Hence, no temperature gradient is left after passage of the scraper blade. This resulted in

$$\alpha_s = \frac{2}{\sqrt{\pi}} (\lambda \rho C_p n N)^{0.5}. \tag{1}$$

This result will be used in the following section, where a model is developed for our purposes. The author underlines that eq. (1) can only be valid in a limited range of *Re* numbers. At low *Re* numbers, when using viscous media, incomplete mixing of the film layer with the bulk decreases the heat transfer coefficient. At high *Re* numbers, the heat transfer coefficient will increase as a result of turbulent eddies disturbing the film layer. He compared his model with the experimental data of Houlton (1944) and Skelland (1958) and concluded that the data of Houlton agreed well with eq. (1), but the data of Skelland did not. The discrepancy between the data of Skelland and eq. (1) was in first instance ascribed to the complex hydrodynamics prevailing in the experiments of Skelland. However, in a later publication Skelland (1962) reported a more reliable correlation which was in satisfactory agreement with eq. (1). Penny and Bell (1967) suggested that axial dispersion probably has played an important role in the data of Skelland because of the low axial flow rates used.

Harriot (1959) also confirmed that liquids having a low viscosity can be described adequately by the penetration model. Viscous media resulted in lower values as predicted by Latinen (1958).

Trommelen (1971) studied flow patterns and heat transfer properties in a scraped surface heat exchanger. He used viscous media (water–glycerol mixtures). He concluded that in the case of Couette flow ($Re_s < 300$) no mixing of the film layer and the bulk takes place after scraping. Also in the transition region ($Re_s > 1000$), where Taylor vortices occur, there is hardly any mixing because of the low penetration depth. His model for heat transfer is based on three steps:

(1) Penetration of heat in a thin stagnant liquid layer between two scraper actions.
(2) Partial equalization of the temperature in that liquid layer remaining temporarily stuck on the scraper blade after it has been scraped off the wall.
(3) Radial transport by convection of the cooled liquid layer into the bulk. This is enhanced by turbulence.

An empirical model was developed based on penetration theory:

$$\alpha = \frac{2}{\sqrt{\pi}} (\lambda \rho C_p n N)^{0.5} \Phi \tag{2}$$

in which Φ is the empirical factor that accounts for axial dispersion and incomplete temperature equalization and mixing (steps 2 and 3). From experimental data he correlated Φ with the Péclet number ($Pé = Re \cdot Pr$), resulting in

$$\Phi = 1 - 2.78(Pé + 200)^{-0.18} \quad (400 < Pé < 6000). \tag{3}$$

In the region where Taylor vortices occur Φ turned out to be constant (0.5).

Nearly all investigations in the literature cited here deal with laminar flow or with the transition region between laminar and turbulent flow. Only Houlton (1944) and Skelland (1958) have reported data with turbulent flow due to high tangential velocities ($Re_s > 10^4$). When scraped-surface heat exchangers are used for crystallization of paraxylene, the flow is fully turbulent due to the high *axial* velocity and low viscosity. For this application, no models have been found in the literature. An extension of the model based on penetration theory [eq. (1)] has been derived for our purpose in the next section.

2.2. *Turbulent pipe flow*

As has become clear from the literature survey, no models are available for the heat transfer coefficient in a scraped-surface heat exchanger in which flow is turbulent because of high axial velocities. In our case we are dealing with a high throughput of a process medium having a low viscosity, resulting in a *Re* number in the order of 10^5, where *Re* is defined as

$$Re = \frac{\rho \langle v \rangle D_h}{\eta} \tag{4}$$

where ρ is the density of the liquid ($kg m^{-3}$), η is the viscosity ($N s m^{-2}$), D_h is the hydraulic diameter (m)

(defined as 4 × cross-section/wetted perimeter) and $\langle v \rangle$ is the mean axial velocity (m/s).

Generally, flow is fully turbulent for $Re > 10{,}000$.

A strongly simplified description of turbulent flow is based on a division of the cross-sectional area of the pipe into two domains:

(1) A turbulent core, with uniform velocity, temperature and concentration profile, which implies that no radial gradients are present in the core.
(2) A boundary layer between the turbulent core and the wall, the thickness of which is dependent on the Re number. In this boundary layer, the radial velocity, temperature and concentration gradients, being the driving forces for transport in radial direction of momentum, heat and mass, respectively, are constant.

For the mathematical description of the presented model for turbulent flow it is necessary to define the boundary layer as that part of the flowing medium where transport by conduction dominates convective transport by turbulent eddies. Because conductive transport of momentum, heat and mass, all have their own characteristic rates expressed in terms of viscosity, thermal conductivity and diffusion coefficient, it will be obvious that the thickness of the boundary layer will be different for each mechanism. The thicknesses of the boundary layers for transport of momentum, heat and mass will be denoted by δ_h, δ_{th} and δ_m, respectively. In this paper, only the transport of momentum and heat will be considered. Mass transport will be treated in a subsequent paper.

Conductive transport of heat can be described by Fourier's law:

$$\dot{Q}_w = -\lambda \frac{dT}{dy} \tag{5}$$

where $\dot{Q}_w$ is the heat flux (W m^{-2}), λ is the thermal conductivity (W m^{-1} °C^{-1}) and dT/dy is the temperature gradient (°C m^{-1}).

In steady-state conditions, the heat flux in radial direction is constant throughout the thermal boundary layer, which implies that the temperature depends linearly on y. Integration of eq. (5) with boundary conditions $y = 0$, $T = T_w$ and $y = \delta_{th}$, $T = T_{bulk}$ yields

$$\dot{Q}_w = \lambda \frac{(T_B - T_w)}{\delta_{th}}. \tag{6}$$

In eq. (6), λ/δ_{th} is defined as the heat transfer coefficient, α.

In the absence of scraper blades, the values of the heat transfer coefficients are estimated by the equation developed by Gnielinski (1975):

$$Nu = \frac{\xi/8(Re - 1000)Pr}{1 + 12.7(\xi/8)^{0.5}(Pr^{2/3} - 1)}\left[1 + \left(\frac{D_h}{L}\right)^{2/3}\right] \times \left(\frac{Pr}{Pr_w}\right)^{0.11} \tag{7}$$

with

$$\xi = (1.82 \log Re - 1.64)^2. \tag{8}$$

This equation is recommended because it takes inlet and outlet effects into account as well as heat production due to friction. It has proven to be capable of sufficiently accurate predictions in the transition region and turbulent flow.

Corrections for flow through an annular space are proposed by Petrukov and Roisen (1964). For heat transfer to the inner tube these authors arrive at

$$Nu = Nu_{tube}\left(\frac{d_a}{d_b}\right)^{0.16} \tag{9}$$

assuming no heat exchange to take place between environment and the outer tube, and for heat transfer to the outer tube:

$$Nu = Nu_{tube}[1 - 0.14(d_b/d_a)^{0.6}] \tag{10}$$

assuming the inner tube to be perfectly insulated. In these equations d_a represents the inner diameter of the outer tube and d_b the outer diameter of the inner tube.

The presence of the scraper blades mechanism is counted for by including the wetting of the blades in the hydraulic diameter, being defined as 4 times the cross-sectional area divided by the wetted perimeter.

2.3. *The influence of the scraper action on the heat transfer coefficient*

The steady state is disturbed by the presence of rotating scraper blades, wiping off the boundary layer with a certain frequency. Complete mixing between the removed boundary layer and the bulk is assumed. Hence, right after the passage of a scraper blade, the temperature of the liquid attached to the wall equals the bulk temperature T_B. From this moment on, a velocity gradient builds up in radial direction, according to the well-known penetration theory (Beek and Mutzall, 1977). A necessary condition for the modelling of heat transfer by penetration theory as well is that the penetration of heat can be regarded as proceeding in a stagnant medium. This situation is approached for penetration of heat in laminar flow, because no disturbance of the temperature profile by turbulent eddies is allowed. In order to fulfill this requirement, the laminar boundary layer has to develop at least as fast as the penetration of heat proceeds. During this penetration period, the ratio of the penetration depths of momentum and heat can be calculated from

$$\frac{\delta_h}{\delta_{th}} = \frac{\sqrt{(\pi \nu t)}}{\sqrt{(\pi a t)}} = Pr^{1/2} \tag{11}$$

and for completely developed boundary layers,

$$\frac{\delta_h}{\delta_{th}} = Pr^{1/3}. \tag{12}$$

From eqs (11) and (12) it appears that the laminar boundary layer, δ_h, is always thicker than the thermal

boundary layer, δ_{th}, when $Pr > 1$. The difference between the exponents of the Pr number in eqs (11) and (12) indicates that, after the blade has passed, the laminar boundary layer develops faster than the thermal boundary layer does. As the condition of $Pr > 1$ is met in our case, as it is in general when the process medium is a liquid, the mathematical description of the development of the temperature profile with penetration theory turns out to be justified.

It will be assumed now that the transport of heat by a temperature gradient in axial direction may be neglected. In this case, the temperature profile across the boundary layer results from solving the well-known equation of Fourier:

$$\frac{\partial T}{\partial t} = \frac{\lambda}{\rho C_p}\frac{\partial^2 T}{\partial y^2} \tag{13}$$

with boundary conditions $y = 0$, $T = T_w$ and $y \to \infty$, $T = T_B$ for $t > 0$ and initial condition $t = 0$, $T = T_B$ for all y. Solution of eq. (13) with the boundary conditions yields

$$\frac{T - T_w}{T_B - T_w} = \frac{2}{\sqrt{\pi}}\int_0^{y/(2\sqrt{at})} e^{-\gamma^2}\,d\gamma. \tag{14}$$

The development of the temperature profile has been illustrated in Fig. 1.

Combination of eqs (5) and (14) expresses the heat flux through the wall as a function of time:

$$\dot{Q}_w = -\lambda\left.\frac{\partial T}{\partial y}\right|_{y=0} = (T_B - T_w)\left(\frac{\lambda\rho C_p}{\pi t}\right)^{0.5}. \tag{15}$$

According to eq. (6) the heat transfer coefficient can be expressed as

$$\alpha(t) = \sqrt{\frac{\lambda\rho C_p}{\pi t}}. \tag{16}$$

When the heat transfer mechanism between two scraper actions can be described with penetration theory, the time-mean value of the heat transfer coefficient can be calculated from

$$\bar{\alpha} = \frac{1}{t_s}\int_0^{t_s} \alpha(t)\,dt. \tag{17}$$

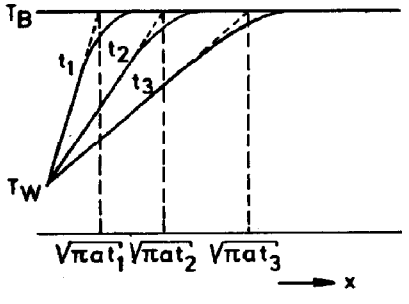

Fig. 1. Development of the temperature profile according to penetration theory.

Combination of eqs (16) and (17) results in

$$\bar{\alpha} = 2\sqrt{\frac{\lambda\rho C_p}{\pi t_s}}. \tag{18}$$

Expressing the time between two scraper actions in terms of the number of blades and the rotational frequency N,

$$t_s = \frac{1}{nN}. \tag{19}$$

Equation (18) combined with eq. (19) yields

$$\bar{\alpha} = \frac{2}{\sqrt{\pi}}(\lambda\rho C_p nN)^{0.5}. \tag{2}$$

This expression has already been derived by Latinen (1958).

So far, the result of the theoretical description for turbulent flow is the same as for laminar flow. This is due to the assumption that the heat transfer process can be described by penetration theory during the entire time interval between two scraper actions. This assumption is only met if the time between two scraper actions is less than the time required for complete penetration of the thermal boundary layer. This means that, for turbulent flow, penetration theory can only be used for rotational frequencies of the scraper above a certain value, so that the time between the scraper blade passages equals or is smaller than the time needed for penetration of the thermal boundary layer. From Fig. 1, it appears that the penetration depth, δ_{th}, equals $\sqrt{\pi\lambda t/\rho C_p}$. Conversely, the time required for full development of the thermal boundary layer equals

$$t_\delta = \frac{\delta_{th}^2 \rho C_p}{\pi\lambda}. \tag{20}$$

In the case of turbulent flow the thickness of the thermal boundary layer, δ_{th}, can be expressed as $\delta_{th} = \lambda/\alpha$. Now, eq. (20) can be converted into

$$t_\delta = \frac{\lambda\rho C_p}{\pi\alpha^2}. \tag{21}$$

With $t_s = 1/nN$ the following expression for the minimum rotational speed results:

$$N_{\min} = \frac{\pi\alpha^2}{n\lambda\rho C_p}. \tag{22}$$

For the xylene mixture with $\lambda = 0.15$ W m^{-1} °C^{-1}, $\rho = 900$ kg m^{-3}, $C_p = 1600$ kJ kg^{-1} K^{-1} the scraper containing two rows of scraper blades and $\alpha_t(\Phi_v) \approx 1000$ W m^{-2} K^{-1} eq. (22) gives $N_{\min} \approx 8$ rev s^{-1}.

In the process we studied rotational speeds of 1 rev s^{-1} are common, which implies that the mathematical description of heat transfer under these circumstances requires an extension of the model treated so far. Therefore, a second assumption is made that after the penetration of heat through the thermal

boundary layer has been completed, the situation is the same as with turbulent pipe flow, until the scraper passes again. The time-mean value of the heat transfer coefficient is expressed by eq. (17) by splitting the integral into two parts:

(1) The first part from $t = 0$ until $t = t_\delta$ when heat transfer is governed by penetration theory.
(2) The second part between t_δ and t_s. During this period, the heat transfer coefficient equals that for turbulent pipe flow under the same conditions without any scraper action.

The time-mean value of the heat transfer coefficient is a function of rotational speed *and* flow rate, because the heat transfer coefficient for turbulent pipe flow depends on the flow rate. Expressed in mathematical terms,

$$\bar{\alpha}(N, \phi_v) = \frac{1}{t_s}\left[\int_0^{t_\delta} \alpha_p(t)\,\mathrm{d}t + \int_{t_\delta}^{t_s} \alpha_t(\phi_v)\,\mathrm{d}t\right] \quad (23)$$

with $\alpha_p(t)$ being the time-dependent heat transfer coefficient during the penetration period and $\alpha_t(\phi_v)$ being the flow-dependent heat transfer coefficient for turbulent pipe flow.

Evaluation of the integrals in eq. (23) using eq. (16) and elimination of t_δ by eq. (21) and t_s by eq. (19) results, after rearranging, in:

$$\bar{\alpha}(N, \phi_v) = \frac{n\lambda\rho C_p}{\pi\alpha_t(\phi_v)} N + \alpha_t(\phi_v). \quad (24)$$

Equation (24) predicts a linear relationship between $\bar{\alpha}(N, \phi_v)$ and N in the region $N = 0 - N_{\min}$ for a given value of $\alpha_t(\phi_v)$. Using eq. (22), it appears from eq. (24) that $\bar{\alpha}(N, \phi_v) = 2\alpha_t(\phi_v)$ when N equals $N_{\min}$. For $N > N_{\min}$ eq. (1) is valid, which implies $\bar{\alpha}(N, \phi_v) \propto \sqrt{N}$. The relationship between $\bar{\alpha}(N, \phi_v)$ and N, with $\alpha_t(\phi_v)$ being treated as parameter, is presented in Fig. 2(a).

The relationship between $\bar{\alpha}(N, \phi_v)$ and $\alpha_t(\phi_v)$, with N being the parameter, is presented in Fig. 2(b). The diagonal line represents the value of $N_{\min}$, where $\bar{\alpha}(\phi_v, N) = 2\alpha_t(\phi_v)$. The entire region on the left side of this line is governed by eq. (1), which means that $\bar{\alpha}(\phi_v, N)$ depends only on N. The region on the right side is described by eq. (24). All lines that represent $\bar{\alpha}(\phi_v, N)$ at constant N will approach the line with $N = 0$ when α_t goes to infinity. Furthermore, it appears that the influence of $\alpha_t(\phi_v)$, and thus of ϕ_v, decreases with increasing rotational speed. This can be seen immediately by differentiation of eq. (24) with respect to ϕ_v:

$$\left[\frac{\partial\bar{\alpha}(N, \phi_v)}{\partial\phi_v}\right]_N = \left[1 - \frac{n\lambda\rho C_p}{\pi\alpha_t^2(\phi_v)} N\right]\frac{\mathrm{d}\alpha_t(\phi_v)}{\mathrm{d}\phi_v}. \quad (25)$$

From eq. (25) it appears that $[\partial\bar{\alpha}(N, \phi_v)/\partial\phi_v]_N < \mathrm{d}\alpha_t(\phi_v)/\mathrm{d}\phi_v$, the difference being more pronounced at increasing values of N.

Figure 2(c) represents eq. (24) by using $\bar{\alpha}(N, \phi_v)$ as parameter. The region at the left side of the line

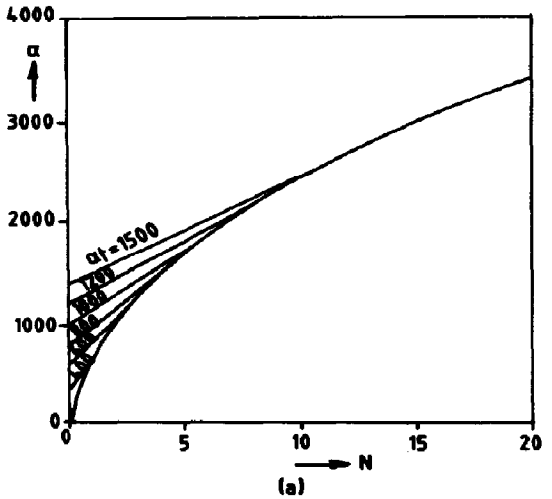

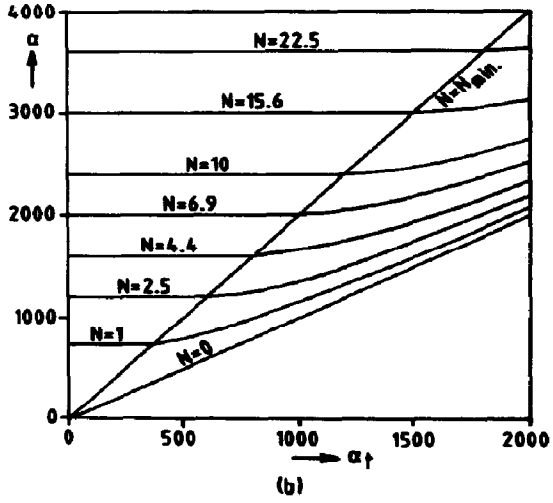

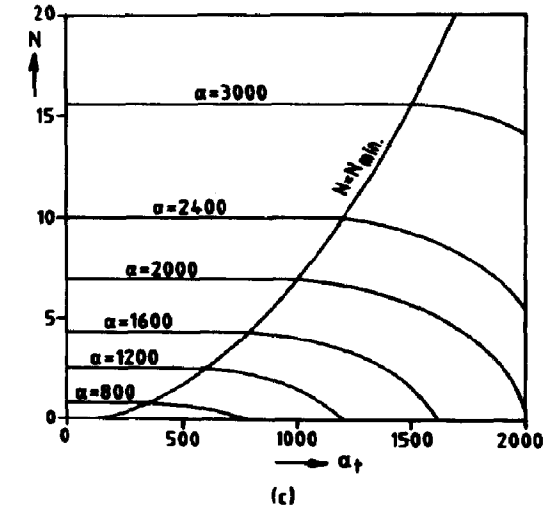

Fig. 2. Graphical representation of eq. (24).

$N = N_{min}$ again is governed by penetration theory only. Each line represents a set of combinations of $\alpha_t(\phi_v)$ and N that result in the same value of $\bar{\alpha}(\phi_v, N)$.

2.4. *The influence of the scraper action on the flow pattern*

So far, it has been assumed that the scraper only removes the boundary layer and that the flow pattern is completely identical to that for turbulent pipe flow. In principle, this treatment is valid only for scraper blades with an infinitely small height. Real scraper blades will influence the flow pattern because of the force they exert upon the surrounding liquid.

To obtain an impression of the disturbance of the flow pattern, a two-dimensional computer simulation has been performed using the PHOENICS-program for the geometry of the bench scale scraped-surface heat exchanger. This procedure involves the numerical solution of the Navier–Stokes equation. The energy dissipation due to turbulent forces is calculated with the k, ε-model (Launder and Spalding, 1974). The results of these calculations are presented in Fig. 3(a) and (b).

These calculations predict the development of a vortex between the scraper blades. It should be noted here that the results have to be interpreted very carefully because the validity of the prediction for the three-dimensional case is questionable. The restriction to two dimensions and, thus, ignoring the effect of the axial velocity has a strong impact on the turbulent properties, which makes the model loose its relevance to a certain extent. A further assumption, which is quite unrealistic, is that of a uniform tangential velocity profile at the entrance of the simulated portion of the two-dimensional scraped-surface heat exchanger. A more realistic simulation was beyond the scope of this paper, but the subject deserves more attention in future. Nevertheless, the results indicate the possible formation of a vortex street in the three-dimensional case. For the modelling of the heat transfer coefficient, the deformation of the boundary layer due to these vortices should be taken into account along the entire surface but, for simplicity, the influence of the vortices shall be treated as additional surface renewal events because each vortex results from a release of the hydrodynamic boundary layer. So, the original surface renewal frequency, nN, should be multiplied by two to take the effect of vortices into account.

3. EXPERIMENTAL

3.1. *Visualization of the flow pattern*

Chemicals. The chemicals required for the visualization of the flow pattern are (all weight percentages):

- —a solution of glycerol in water, 90%,
- —a mixture of 10% 0.3 N NaOH solution in water and 90% glycerol,
- —a mixture of 10% 0.3 N H_2SO_4 solution in water and 90% glycerol,
- —a 1% solution of phenolphtalein in ethanol.

Equipment. The experiments were carried out in a cell that simulates a cross-section of the original scraped-surface heat exchanger. A schematic drawing with the main dimensions is presented in Fig. 4.

Both bottom and top of the cell are made of glass. Illumination is performed with a 1000 W lamp having a colour temperature of 2800 K. The light is reflected by a mirror above the cell to obtain a better distribution of the light falling through the cell. The transmitted light is reflected again by another mirror that is mounted beneath the cell. The normal of the mirror makes an angle of 45° with the axis of the cell. Photographs were taken with a Nikon camera with a two-dimensional lense using a Kodak T-max Professional 400 ASA-film.

Procedure. The scraper cell was filled with 350 ml of the water–glycerol mixture. To this mixture, 10 ml of the NaOH–glycerol mixture and 5 ml phenolphtaleine solution were added. The scrapers are put into action and the colour of the liquid slowly gets pink. During this colouring, the flow pattern is visible. The experiment can be repeated by adding 10 ml of the H_2SO_4–glycerol mixture, making the liquid gradually colourless again. The experiments were performed at a scraper rotational frequency of 0.5 rev s^{-1}. At higher rotational speeds, the colouring proceeded too fast.

3.2. *Measurement of heat transfer coefficient*

Chemicals. The C8-aromatic mixture used for the experimental work was prepared by mixing reformer feed from the EXXON plant (reformer feed is the remaining C8-aromatic mixture *after* partial removal of *p*-xylene) with pure *p*-xylene. Analysis with gas chromatography using a bentonite column revealed the following composition: *p*-xylene 31.78%, metaxylene 38.69%, orthoxylene 9.81%, ethylbenzene 19.45%, toluene 0.27%.

The criterion for choosing a coolant was a maximum value of its heat transfer coefficient at such a flow rate that the uptake of heat could be measured with acceptable accuracy. Methanol, ethanol, pentane, hexane, aceton, chloroform, methylenechloride and trichloroethylene were compared. Due to its low viscosity and high density, resulting in a relatively high Re number, methylenechloride appeared to be the best choice for our purposes. The methylenechloride used was purchased from Vos Chemproha, technical pure grade.

Equipment. The scraped-surface heat exchanger consists of two cylindrical steel tubes with a centre shaft on which the scraper blades are mounted. The coolant flows through the annular space between the cylindrical tubes, while the xylene flows countercurrently through the inner cylinder. Teflon scraper blades are pressed against the wall by springs. These scraper blades are mounted in pairs, the blades differing 180° in angular position. Each pair is rotated 90°

in position with respect to the foregoing–following pair. An illustration with the dimensions of the scraped-surface heat exchanger used for our experiments is presented in Fig. 5.

A schematic representation of the complete configuration is presented in Fig. 6. The coolant circulates with a flow rate of 2 $m^3 h^{-1}$. The xylene flow could be varied between 1–6.6 $m^3 h^{-1}$. The flow rates were

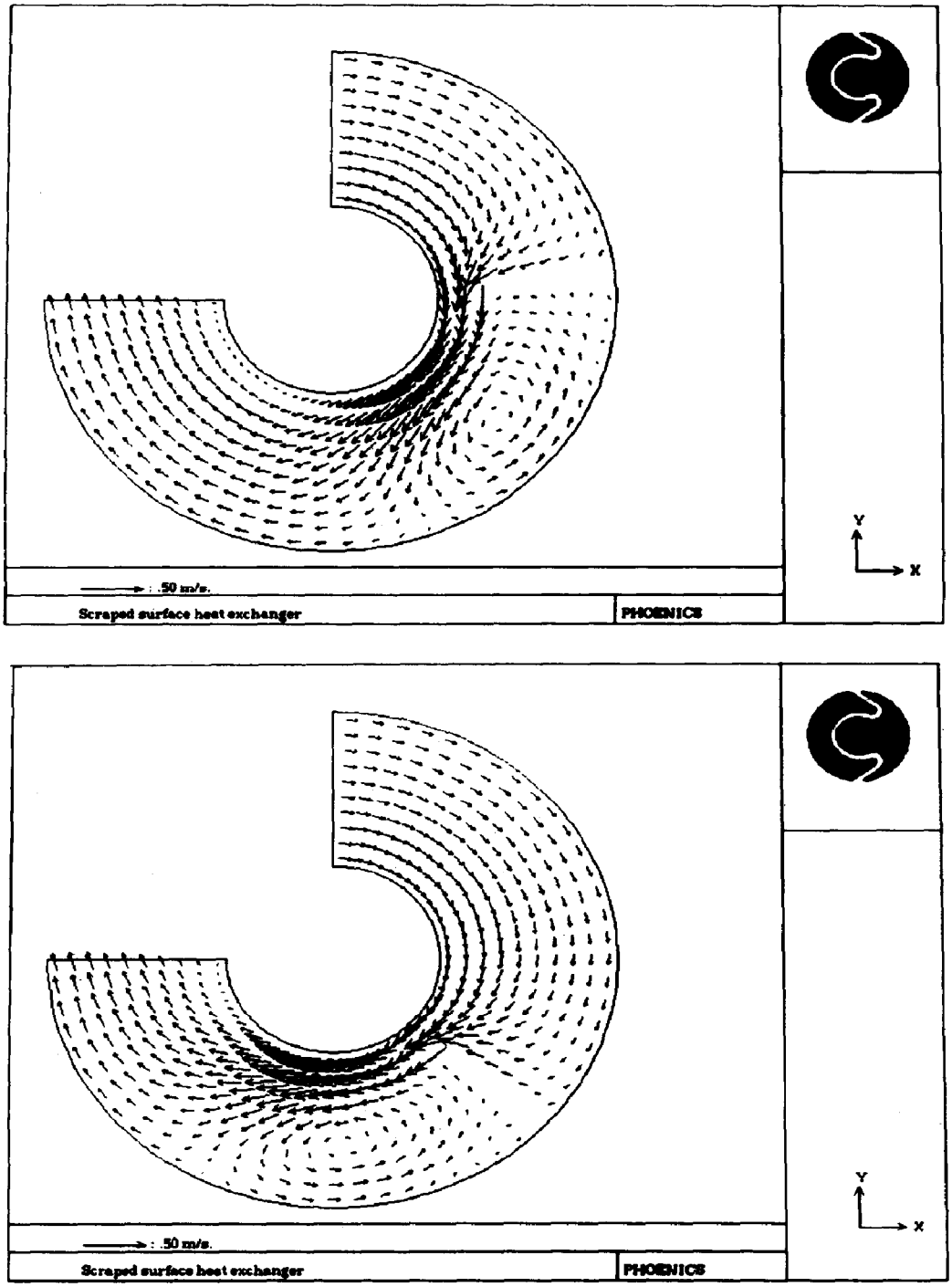

Fig. 3(a) and (b). Cross-sectional flow pattern calculated with the PHOENICS-program for two different positions of the scraper blade.

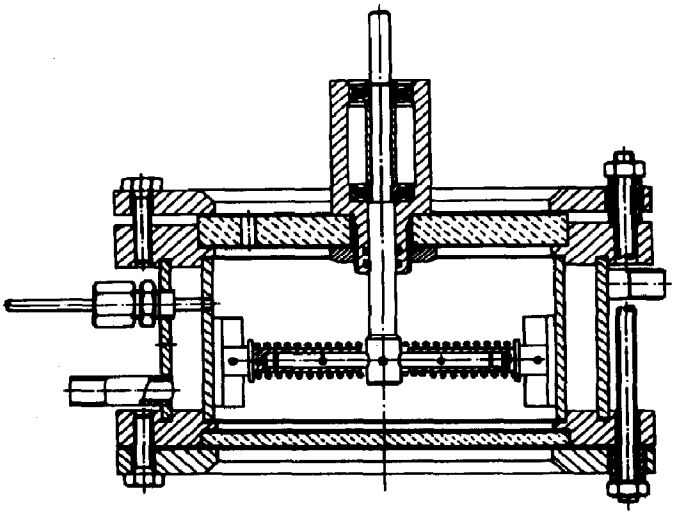

Fig. 4. A schematic representation of the device used for visualization of the flow pattern.

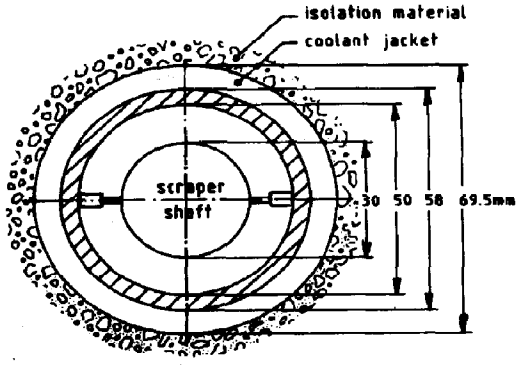

Fig. 5. Cross-section of the bench scale scraped-surface heat exchanger. The length amounts 1 m.

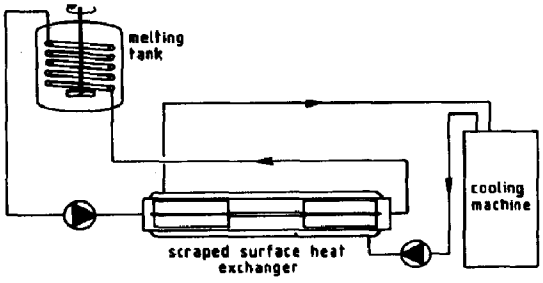

Fig. 6. Schematical drawing of the experimental set-up.

measured with rotameters. The xylene is heated in a stirred vessel, on which the xylene flows through a spiral. Water was used as the heating medium. The temperature of the heating bath was kept at 0–1°C. Temperatures at the inlets and outlets of the scraped-surface heat exchanger were measured with Pt-100 elements, except for the inlet temperature of the coolant. This value was determined by a chromel–alumel thermocouple measuring the difference between the inlet and outlet temperatures of the coolant. This allows for a more accurate determination of the temperature rise and, hence, of the heat flux. The heat flux is always calculated at the coolant side because the temperature drop of the xylene flow becomes too small at high flow rates. All piping and the scraped-surface heat exchanger were insulated in order to minimize heat exchange with the environment.

Procedure. After the cooling bath had reached the desired value, circulation of coolant and xylene was started. The temperatures were monitored. After having reached a steady state, the temperatures and flow rate of the xylene were registered. This procedure was repeated 5–10 times with a time interval of 3 min in order to weigh out fluctuations. Then the flow rate of the xylene was adjusted to another value and, after a steady state was reached again, another measurement was done.

The first series of measurements was performed without scraper blades, in order to check whether our system obeys the predictions of heat transfer coefficients for turbulent flow through an annulus by empirical correlations from the literature.

The second series of measurements was performed with non-rotating scraper blades in order to investigate the influence of the presence of the blades. After these series, measurements were performed with rotational speeds of 0.5 and 1 rev s^{-1}.

3.3. *Data deduction*

From the measured values of the temperatures and flow rates, the value of the overall heat transfer coefficient can be calculated from

$$U = \frac{\dot{Q}_w}{(\Delta T)_{\ln}}. \tag{26}$$

(a)

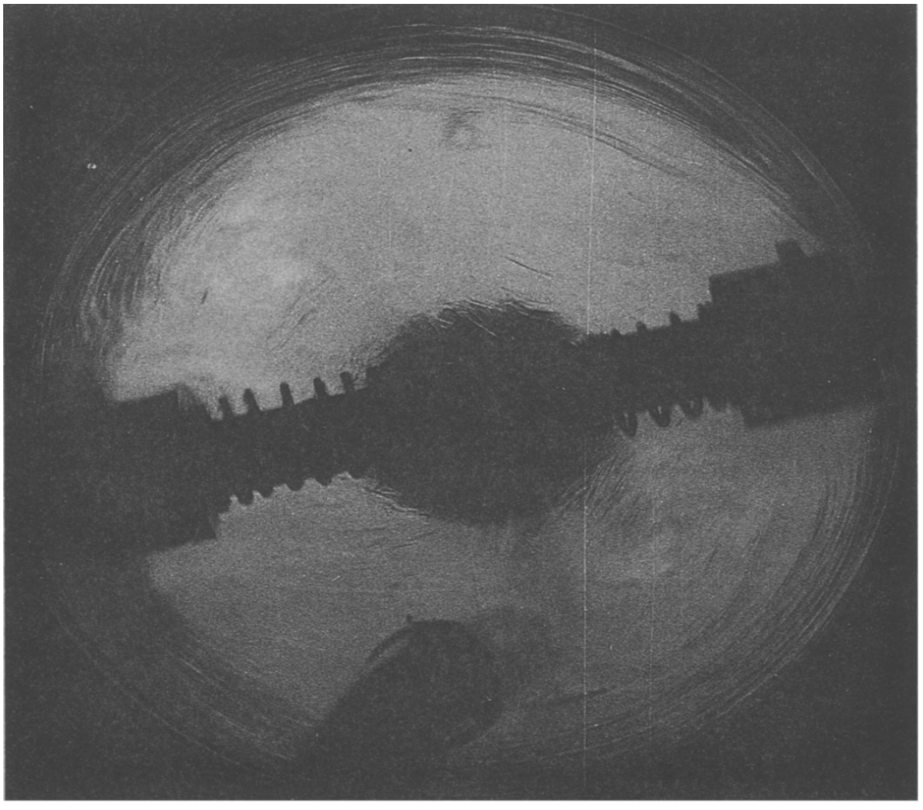

(b)

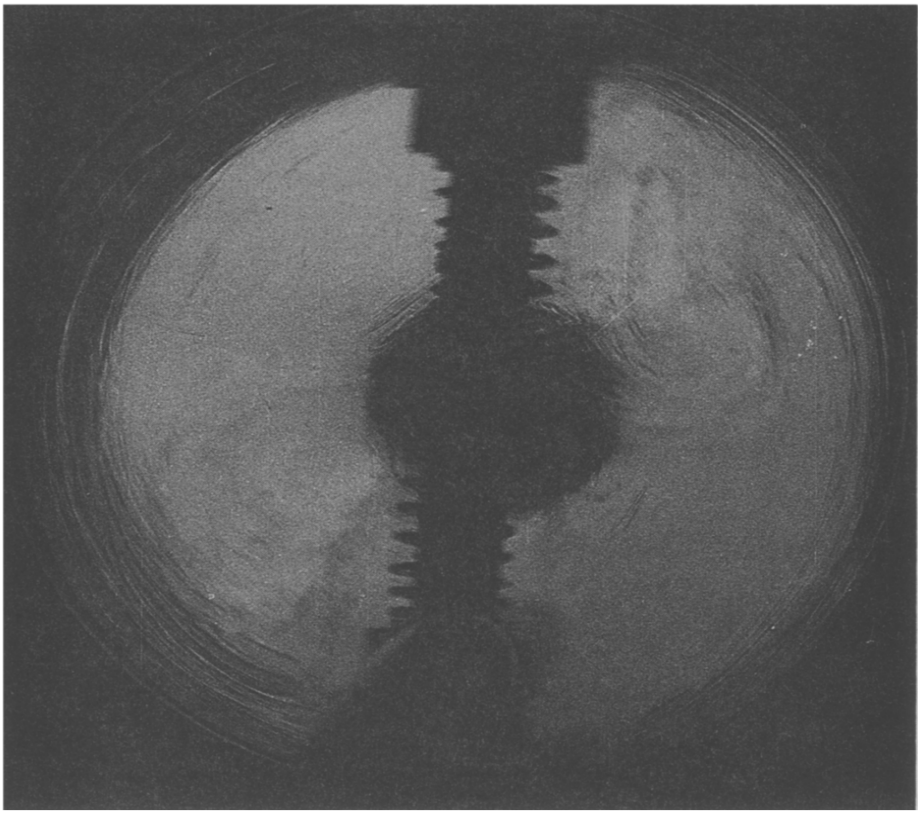

Fig. 7. (a)–(b).

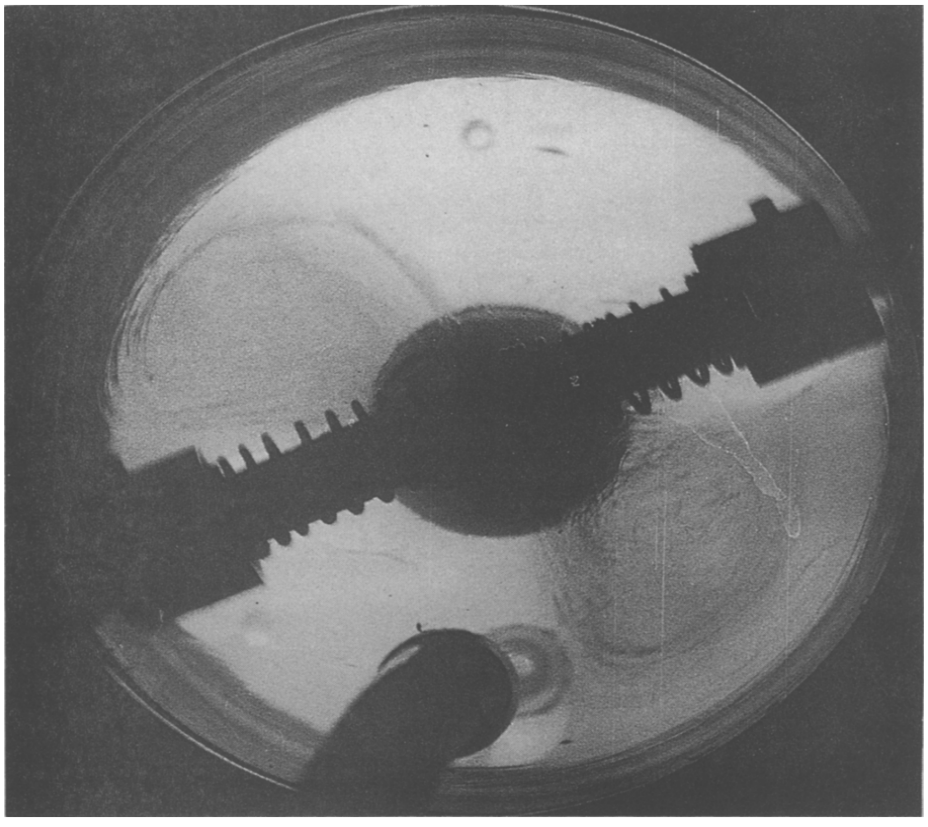

(c

Fig. 7. Photographs of the flow-pattern at $t = 15$, 30 and 120 s, respectively.

The heat flux was calculated from the temperature rise of the coolant and the outer surface of the inner steel tube:

$$\dot{Q}_w = \frac{\phi_{v,k}\,\rho_k C_{pk}(T_{k,\text{out}} - T_{k,\text{in}})}{A}. \tag{27}$$

The logarithmic mean temperature difference is defined as

$$(\Delta T)_{\ln} = \frac{\Delta T_{\max} - \Delta T_{\min}}{\ln(\Delta T_{\max}/\Delta T_{\min})} \tag{28}$$

with $\Delta T_{\max} = T_{\text{xylene, out}} - T_{\text{coolant, in}}$ and $\Delta T_{\min} = T_{\text{xylene, in}} - T_{\text{coolant, out}}$.

From the overall heat transfer coefficient the heat transfer coefficient at the xylene side can be calculated using

$$\frac{1}{U} = \frac{d_u}{d_i}\frac{1}{\alpha_x} + \frac{1}{\alpha_c} + \frac{d_u \ln(d_u/d_i)}{2\lambda} \tag{29}$$

where d_i and d_u are the inner and outer diameters of the pipe, α_x and α_c the heat transfer coefficients of xylene and coolant, respectively, and λ the thermal conductivity of steel. In the case of removed scraper blades, the heat transfer coefficients at both sides are estimated with Gnielinski's equation, presented in Section 2.2.

4. RESULTS AND DISCUSSION

4.1. *Visualization of the flow pattern*

In Fig. 7, three photographs of the flow pattern have been presented at $t = 15$, 30 and 120 s ($t = 0$ is the moment at which the scraper is put into action).

On the presented photographs, the scrapers rotate clockwise and the results clearly indicate the formation of a vortex between the two scraper blades. The motion of the scraper blade presumably causes the frictional forces at the wall in front of the scraper blade to be very high. This results in a release of the laminar boundary layer from the wall. Although the viscosity of the water–glycerol mixture is much higher than that of the xylene mixture, the experimental results agree very well with the prediction presented in Section 2.4. Both procedures indicate that the scraper action induces two "surface renewal events": one due to the scraper blade itself and the other due to the vortex between the scraper blades, resulting from the force exerted upon the boundary layer by the scraper blade.

4.2. *Heat transfer coefficients*

The measured values of the overall heat transfer coefficients with removed scraper blades are presented as a function of the Reynolds number in axial direc-

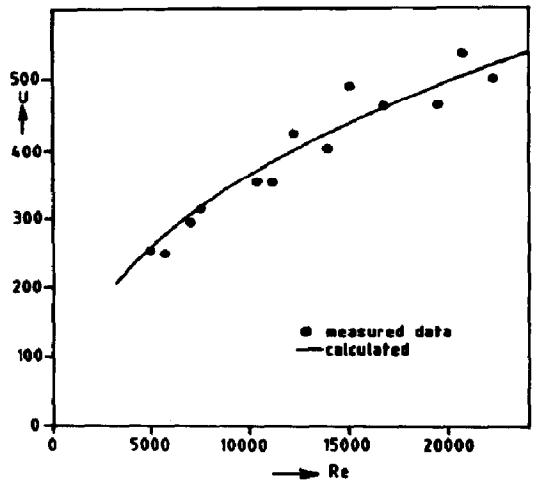

Fig. 8. Measured values of the overall heat transfer coefficients in case of removed scraper blades, compared with calculated values according to Gnielinski's equation.

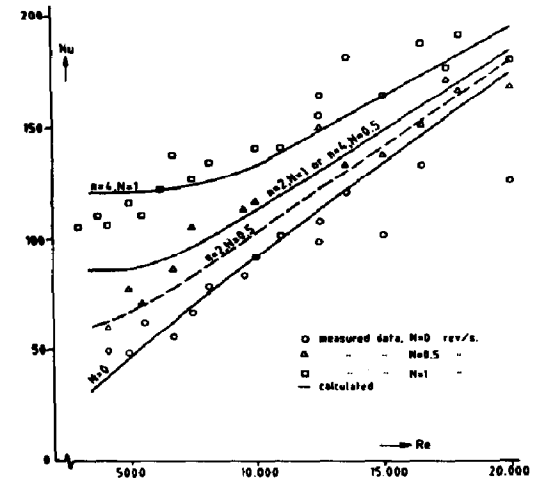

Fig. 9. The heat transfer coefficients at the scraped side as calculated from the measured overall heat transfer coefficients with $N = 0$, $N = 0.5$ and $N = 1$ rev s^{-1}. The solid lines are calculated with eq. (24), using Gnielinski's equation for $\alpha_t(\phi_v)$.

tion in Fig. 8. The solid line represents the overall heat transfer coefficients calculated with Gnielinski's equation, adapted for annular flow. Physical properties are summarized in the Appendix.

From Fig. 8 it appears that the system with removed scraper blades can be adequately described by Gnielinski's equation. For this reason the calculated value of the heat transfer coefficient of the coolant was chosen for further data reduction ($\alpha_c = 920$ W m^{-2} K^{-1}).

The heat transfer coefficients calculated from the overall heat transfer coefficients for $N = 0$, 0.5, 1 rev s^{-1} are presented in Fig. 9. The solid lines represent eq. (24), with $\alpha_t(\phi_v)$ calculated according to Gnielinski's equation.

From Fig. 9 it becomes clear that although scraper blades are present the heat transfer coefficient calculated from experimental data is still in good agreement with the values calculated with Gnielinski's equation. The enhancement of the heat transfer coefficient by the scraper action, however, is significantly larger than predicted by the model derived in Section 2.3. At a rotational speed of 1 rev s^{-1}, the heat transfer coefficient increases by 200% at $Re = 5000$ to 30% at $Re = 20{,}000$, with respect to the situation without any scraper action. This is probably due to the fact that the movement of the scraper blades generates vortices and, hence, decreases the thickness of the laminar boundary layer, which in turn results in a further enhancement of the time-mean value of the heat transfer coefficient. Multiplication of the surface renewal frequency by two, as was proposed to account for the influence of vortices, gives a much better agreement between theory and experiment. This observation indicates that vorticity contributes significantly to the enhancement of the heat transfer coefficient. For this reason, an extensive study on flow phenomena, by numerical simulation as well as experiments, is recommendable.

5. CONCLUSIONS

From the foregoing results the following conclusions can be drawn:

- In the absence of scraper blades, experimental heat transfer data match sufficiently well with predicted values according to Gnielinski's equation, applying corrections for the geometry proposed by Pethukov and Roisen.
- The first conclusion is also valid for the situation with non-rotating scraper blades. This proves that adaption of the Re number for the presence of the blades has not been superfluous; ignoring this influence would result in Re numbers that are 10% higher and, hence, the agreement between theory and experiment would be worse.
- The enhancement of the heat transfer coefficient due to the scraper action can be predicted well with our model. However, the model has to be extended to take the influence of the scraper blades on hydrodynamic properties into account.
- Application of scrapers to increase heat transfer has proven to be very useful for the Re number region we have studied.

NOTATION

a	thermal diffusivity, m^2 s^{-1}
A	surface, m^2
C_p	heat capacity at constant pressure, J kg^{-1} K^{-1}
d, D	diameter, m

n	number of rows of scraper blades, dimensionless
N	rotational frequency, s^{-1}
Q	heat flux, $W\,m^{-2}\,s^{-1}$
t	time, s
T	temperature, °C, K
v	velocity, $m\,s^{-1}$
y	distance from the wall, m

Greek letters

α	heat transfer coefficient, $W\,m^{-2}\,°C^{-1}$
δ	thickness of the boundary layer, m
η	viscosity, $kg\,m^{-1}\,s^{-1}$
λ	thermal conductivity, $W\,m^{-1}\,°C^{-1}$
ρ	density, $kg\,m^{-3}$
ϕ	volume flow, $m^3\,s^{-1}$
Φ	empirical correlation factor, dimensionless

Subscripts

a, b	refer to inner tube and outer tube
B	bulk
c	coolant
h	hydraulic
i	inside
p	penetration
s	scraper
t	turbulent
w	wall
x	xylene

REFERENCES

Beek, W. J. and Mutzall, K. M. K., 1977, *Transport Phenomena*. Wiley, New York.

Gallant, R. W., 1968, *Physical Properties of Hydrocarbons*. Gulf Publishing Company, Houston.

Gnielinski, V., 1975, Neue Gleichungen für den Wärme- und den Stoffübergang in turbulent durchströmten und Kanälen. *Forsch. Ing.-Wes.* **41**(1), 8–16.

Harriott, P., 1959, Heat transfer in scraped surface heat exchangers. *Chem. Engng Prog. Symp. Ser.* **29**, 137–139.

Houlton, H. G., 1944, Heat transfer in the votator. *Ind. Engng Chem.* **36**, 522–528.

Huggins, F. E., 1931, Effect on scrapers on heating, cooling, and mixing. *Ind. Engng Chem.* **23**, 749–753.

Latinen, G. A., 1958, Discussion of the paper "Correlation of scraped-film heat transfer in the votator" (A. H. Skelland). *Chem. Engng Sci.* **9**, 263–266.

Launder, B. E. and Spalding, D. B., 1974, *Comput. Meth. Appl. Mech. Engng* **3**, 269–289.

Penney, W. R. and Bell, K. J., 1967, Close-clearance agitators. Part 2. Heat transfer coefficients. *Ind. Engng Chem.* **59**, 47–54.

Petukhov, B. S. and Roizen, L. I., 1964, Generalized relationships for heat transfer in a turbulent flow of gas in tubes of annular section. *High Temperature* **2**, 65–68.

Skelland, A. H. P., 1958, Correlation of scraped-film heat transfer in the votator. *Chem. Engng Sci.* **7**, 166–175.

Skelland, A. H. P., Oliver, D. R. and Tooke, S., 1962, Heat transfer in a water–cooled scraped surface heat exchanger. *Br. chem. Engng* **7**, 346–353.

Trommelen, A. M. and Beek, W. J., 1971, Flow phenomena in a scraped-surface heat exchanger ("votator"-type) *Chem. Engng Sci.* **26**, 1933–1942, 1977–2001.

APPENDIX: RELEVANT PHYSICAL PROPERTIES

Coolant

The relevant physical properties of methylenechloride at −30°C were taken from Gallant (1968):

$$\rho = 1402.6\ kg\,m^{-3}, \qquad C_p = 1141.1\ J\,kg^{-1}\,K^{-1}$$

$$\lambda = 0.1589\ W\,m^{-1}\,K^{-1}, \qquad \eta = 0.74 \times 10^{-5}\ N\,s\,m^{-2}.$$

Process medium

The relevant physical properties of the C8-aromatic mixture were calculated with the program "Process", and fitting as a function of temperature resulted in the following equations (T in K):

$$\rho = 1100.4 - 0.8807T \qquad (kg\,m^{-3})$$

$$C_p = 3.5882T + 616.2 \qquad (J\,kg^{-1}\,K^{-1})$$

$$\eta = \exp(-10.738 + 988.67T) \qquad (N\,s\,m^{-2})$$

$$\lambda = 0.1943 - 0.000213T \qquad (W\,m^{-1}\,K^{-1}).$$